Acta Cryst. (1985). A**41**, 158–163

Lattice Dynamical Calculation of First-Order Thermal Diffuse Scattering in Phenothiazine

BY A. CRIADO,* A. CONDE AND R. MÁRQUEZ

Departamento de Optica y Sección de Física del Centro Coordinado del CSIC, Universidad de Sevilla, Spain

(*Received* 30 *April* 1984; *accepted* 3 *October* 1984)

Abstract

A computer program has been developed to calculate first-order thermal diffuse scattering (TDS) intensity from eigenvectors and eigenvalues of the dynamical matrix obtained within the harmonic approximation with an atom–atom potential function and the external Born–von Kármán formalism. It is applied to monoclinic phenothiazine and correction factors of Bragg intensities due to TDS contribution are calculated and compared with the long-wave approximation. A Fourier difference synthesis is performed in order to reveal the influence of TDS contributions in electron density maps. A least-squares process is carried out to obtain the changes in structural parameters due to TDS contribution.

Introduction

The interaction between monochromatic X-ray radiation, with wave vector **K**, and an ideal crystal can be described by diffracted beams with wave vectors **K**′, such that $\mathbf{K}'-\mathbf{K}=\mathbf{G}$ and $\mathbf{G}=2\pi\mathbf{H}$, where **H** is a reciprocal vector of the crystal (hereafter, we will refer to **G** vectors as reciprocal space, for the sake of conciseness), and this is known as Bragg diffraction. The effect of lattice vibrations, present at a given temperature, over the Bragg diffraction peaks is a variation, usually decreasing, of their intensities.

Simultaneously, lattice vibrations cause the appearance of inelastic scattered intensity in regions different from reciprocal-lattice points. This intensity is known as thermal diffuse scattering (TDS) radiation and from a quantum-mechanical point of view can be interpreted as the interaction of incident photons with elementary excitation quanta, phonons. The interaction with only a phonon with wave vector **q** is known as first-order TDS and gives rise to scattering intensity at points that differ from the reciprocal-lattice point by a **q** vector. Similarly, interactions with more than one phonon are known as second-order (two phonons) and, in general, multiphonon processes.

The knowledge of thermal diffuse scattering is important in crystal structure analysis and especially in high-precision work such as electron density studies because experimental Bragg intensities are measured by scanning a small reciprocal volume around each reciprocal-lattice point and therefore a determined inelastic contribution is present in the measurement. There is no conventional experimental way of rejecting this intensity and energy discrimination would be useless because changes in frequency are negligible. The most effective way is a theoretical calculation of TDS intensity by means of a suitable lattice dynamical model or in the long-wave (LW) approximation and its subtraction from experimental measurements.

Basic theory

The theory of thermal diffuse scattering is widely reproduced by several authors (Cochran, 1963; Maradudin, Montroll, Weiss & Ipatova, 1971; Cochran & Pawley, 1964) and we will present here only the main results. The first-order TDS intensity at a point **S** of the reciprocal space differing by **q** from a reciprocal-lattice point is given by

$$\frac{\mathrm{d}I_1(\mathbf{S}=\mathbf{G}-\mathbf{q})}{\mathrm{d}\mathbf{q}}=NS^2\sum_j\frac{E_j(\mathbf{q})}{\omega_j^2(\mathbf{q})}|F_1(\mathbf{S},\mathbf{q}j)|^2,$$

where j stands for the different crystal modes with wave vector **q**, $\omega_j(\mathbf{q})$ is the angular frequency of mode $(\mathbf{q}j)$, $E_j(\mathbf{q})$ is its energy (k_BT in the high-temperature limit) and $F_1(\mathbf{S},\mathbf{q}j)$ is the first-order structure factor. It can be seen that modes with low frequency contribute more intensely, so if we are dealing with a molecular crystal, where internal and lattice modes are very different in frequency ranges, we can neglect the internal contribution and treat the molecule as a rigid body within the external Born–von Kármán formalism of lattice dynamics. In this case the expression for the first-order structure factor is

$$\begin{aligned}F_1(\mathbf{S},\mathbf{q}j)=\sum_k\sum_i\{&f_{ki}(\mathbf{S})T_{ki}(\mathbf{S})\\&\times\mathbf{s}[\mathbf{e}''(\mathbf{q}|kj)+\mathbf{e}'''(\mathbf{q}|kj)\times\mathbf{x}(ki)]\\&\times\exp[i\mathbf{S}\,.\,\mathbf{x}(ki)]\exp[i\mathbf{G}\,.\,\mathbf{x}(k)]\},\end{aligned}$$

where k and i represent different molecules in the unit cell and different atoms in a molecule respectively, $f_{ki}(\mathbf{S})$ is the atomic scattering factor of atom

* This work forms part of the doctoral thesis submitted to the Universidad de Sevilla.

0108-7673/85/020158-06$01.50

ki, $T_{ki}(\mathbf{S})$ is the temperature factor (Willis & Pryor, 1975) of atom ki, $\mathbf{s}$ is a unit vector along the direction of $\mathbf{S}$, $\mathbf{x}(k)$ is the position vector of the centre of mass of molecule k and $\mathbf{x}(ki)$ is the position vector of atom i belonging to molecule k with respect to its centre of mass.

Lattice modes can be obtained by solving the eigenvalue equation as the eigenvalues and eigenvectors of the dynamical matrix $D(\mathbf{q})$ (Born & Huang, 1968; Maradudin & Vosko, 1968), which yields $6Z$ modes for a given $\mathbf{q}$, Z being the number of molecules in the unit cell;

$$D(\mathbf{q})\mathbf{U}(\mathbf{q}) = \omega^2(\mathbf{q})\mathbf{U}(\mathbf{q})$$

using mass-weighted external coordinates and local coordinate systems coinciding with the principal inertia axes of each molecule. $\mathbf{e}''^{t}(\mathbf{q}|kj)$ and $\mathbf{e}''^{r}(\mathbf{q}|kj)$ are the mass-unweighted components, translational and rotational, of $(\mathbf{q}j)$ lattice mode displacements relative to molecule k and can be obtained as

$$\mathbf{e}'^{t}_{\alpha}(\mathbf{q}|kj) = m(k)^{-1/2}\mathbf{e}^{t}_{\alpha}(\mathbf{q}|kj)$$
$$\mathbf{e}'^{r}_{\alpha}(\mathbf{q}|kj) = I^{-1/2}_{\alpha}(k)\mathbf{e}^{r}_{\alpha}(\mathbf{q}|kj),$$

where α means x, y and z components, $m(k)$ is the mass of molecule k, $I_\alpha(k)$ is the principal inertial moment of k along direction α and $\mathbf{e}(\mathbf{q}|kj)$ is an eigenvector of the dynamical matrix normalized to unity.

The intensity in Bragg peaks corresponding to elastic scattering is given by

$$I_{\text{Bragg}}(\mathbf{G}) = [(2\pi)^3/V_c]N|F(\mathbf{G})|^2,$$

where V_c is the unit-cell volume, $F(\mathbf{G})$ the structure factor

$$F(\mathbf{G}) = \sum_k \sum_i f_{ki}(\mathbf{G})\, T_{ki}(\mathbf{G}) \exp\{i\mathbf{G} \cdot \mathbf{x}_k(i)\}$$

and $\mathbf{x}_k(i)$ is the position of atom i situated in molecule k with respect to a fixed crystal frame.

The most important contribution to the first-order TDS occurs in the vicinity of the reciprocal-lattice points and comes from the acoustic modes, which present the property of having zero frequencies in the limit $q \to 0$. In this limit the long-wave approximation is applicable (Born & Huang, 1968), where the relation between frequencies and wave vectors is linear and the polarization components of eigenvectors for the different atoms in the unit cell are real and equal and depend only on the wave-vector direction. This implies that rotational components are zero in the external formalism. Using this approximation, the first-order TDS intensity adopts the following simplified form:

$$\frac{\mathrm{d}I_1(\mathbf{S}=\mathbf{G}-\mathbf{q})}{\mathrm{d}\mathbf{q}} = NS^2|F(\mathbf{G})|^2 \sum_{j_{ac}} \frac{E_j\mathbf{q})}{\omega_j^2(\mathbf{q})} \{\mathbf{s} \cdot \mathbf{e}'^{\mathrm{LW}}(\mathbf{q}j)\}^2.$$

In this limit, crystal waves are elastic, they can be obtained from the elastic constants of the crystal, and are the most common source of information about diffuse scattering near the reciprocal-lattice points.

Method of calculation

In this work the monoclinic variety of phenothiazine was chosen as a subject of our study because an atom–atom potential model described in a previous paper (Criado, Conde & Márquez, 1984) has been successful in the calculation of the thermal crystallographic parameters at 300 K for this compound, in good agreement with experimental ones.

We have written a Fortran program that calculates the first-order TDS intensity at any point of reciprocal space. It uses a previously written program (Criado, Conde & Márquez, 1984), which obtains the dispersion curves of a molecular crystal using an atom–atom potential function in the form $V(r) = -A/r^6 + B \exp(-Cr)$, together with the thermal crystallographic parameters and the temperature factors. Eigenvalues and eigenvectors of the dynamical matrix can be obtained for sufficiently dense sampling through the Brillouin zone and are stored on a magnetic tape. From these data, the program can calculate the first-order structure factor and the TDS intensity for any point in the reciprocal space. A long-wave approximation has also been set up in the LWD version (Kroon & Vos, 1979), *i.e.* using the LW expressions but utilizing the true values of $\omega_j(\mathbf{q})$ given by the lattice-dynamics calculations.

Atomic scattering factors were taken from *International Tables for X-ray Crystallography* (1974) and a polynomial interpolation procedure was employed. The Brillouin zone was sampled by dividing each basic reciprocal vector into 25 parts, and storing the eigenvalues and vectors of the dynamical matrix for half a Brillouin zone, since the other half can be obtained through the time-reversal relations (Venkataraman & Sahni, 1970)

$$\omega(\mathbf{q}) = \omega(-\mathbf{q})$$
$$\mathbf{e}(\mathbf{q}) = \mathbf{e}^*(-\mathbf{q}).$$

The calculated lattice-dynamical crystallographic parameters at 300 K and the energy-minimized crystal configuration (Criado, Conde & Márquez, 1984) were also stored.

Results

First-order TDS intensity

In Fig. 1, we present the calculated first-order TDS intensity along the symmetry direction $\mathbf{b}^*$, where, following the nomenclature of Kroon & Vos (1979), EX is the exact lattice-dynamical value calculated from the 12 dispersion branches and LWD is the value calculated in the long-wave approximation

allowing for dispersion. Divergent behaviour can be seen near the reciprocal-lattice points due to the acoustic contribution, though its integral over a volume is finite. The decrease of I_1(TDS) with S is due to the contribution of the temperature factor in the first-order structure factor, which counteracts the S^2 behaviour. In Fig. 2, the intensity through a chosen reflection along **b*** is separated into acoustic and optical contributions, the optical contribution being approximately constant through the reciprocal-lattice point, and the LWD approximation attains identical values to those of the EX calculation for points near the reciprocal points. The well behaviour of the optical contribution may originate from the fact of the higher frequencies in the centre of the Brillouin zone with respect to the zone frontier in optical branches, considering the average over all branches and directions.

Bragg intensities first-order correction factors

When a given volume around a reflection is scanned, the non-uniform character of the TDS intensity means that its contribution is not cancelled with the measurement of the background and a net intensity is added to the Bragg contribution. This net intensity can be calculated by (Willis & Pryor, 1975)

$$I_1(\mathbf{G}) = \int_{V_p(\mathbf{G})} I_1(\mathbf{S})\,\mathrm{d}\mathbf{S} - \frac{V_p(\mathbf{G})}{V_b(\mathbf{G})} \int_{V_b(\mathbf{G})} I_1(\mathbf{S})\,\mathrm{d}\mathbf{S},$$

where $V_b(\mathbf{G})$ and $V_p(\mathbf{G})$ are the volumes scanned in reciprocal space to measure the background and the peak contributions. These volumes are not equal for the different reflections, and depend on the kind of scan performed (Helmholdt & Vos, 1977) and on the orientation of the crystal with respect to the diffractometer axes (Busing & Levy, 1967). We do not know these experimental conditions for the crystal analysis of phenothiazine (Bell, Blount, Briscoe & Freeman, 1968) and we have chosen a constant symmetric scan volume consisting of a parallelepiped centred on the reflection with seven divisions along each edge, *i.e.* 7/25 of the corresponding basic reciprocal vector. This parallelepiped has a volume of 46 pm^{-3} in **H** reciprocal space; for the experimental conditions chosen by Helmholdt & Vos (1977) with an ω scan of 2° the volume is 48 pm^{-3} for a reflection with $\sin\theta/\lambda = 1{\cdot}0$ Å^{-1}. Thus, the present volume is sufficient to obtain a good approximation to a practical case. The background intensity has been calculated with one more division on each side along **a***. The functional form of first-order TDS depends, in the long-wave limit, on q^{-2}, so a problem arises when we calculate the integral of the element centred on the origin. For calculating this contribution, the method of Kroon & Vos (1978), used by us in the calculation of thermal parameters for phenothiazine (Criado, Conde & Márquez, 1984), has been utilized, where the $q \to 0$ element contribution is obtained from those of the surrounding elements and an empirical factor η, which multiplies this contribution, is introduced to correct numerical errors. This parameter was found to be $\eta = 1{\cdot}38$. Nevertheless, in TDS calculation, this integral is not extended to the whole Brillouin zone, and each parallelepiped is divided into a small number of volume elements, so η must be adjusted to the number of divisions used. The adjustment has been performed to calculate the integral of q^{-2} over a parallelepiped with dense sampling, using the same process with a sampling of $(2n+1)$ divisions along each side and comparing results. In Table 1 we can see η values for different values of n, the $n = \infty$ value corresponds to the one used in thermal parameters and the $n = 0$ value to the correction to be applied to the contribution of a sphere inscribed in the $q = 0$ element to obtain the contribution of this element.

In this way we have calculated optical and acoustic contributions at 300 K to measured intensities for a set of chosen reflections, which are shown in Table 2, together with the structure factors. It can be observed, in agreement with Fig. 2, that the optical contribution is very small because the peak contribution is cancelled with background measurement and, practically, the contribution arises from acoustic modes. The negative value of I_1(opt) is related to the

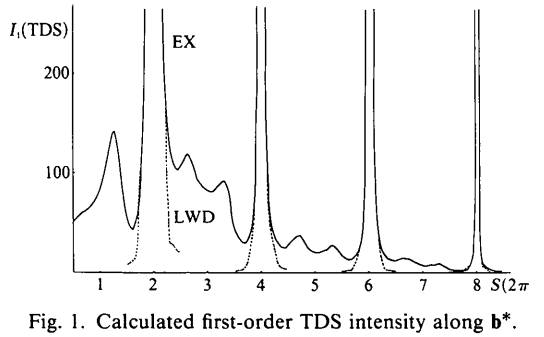

Fig. 1. Calculated first-order TDS intensity along **b***.

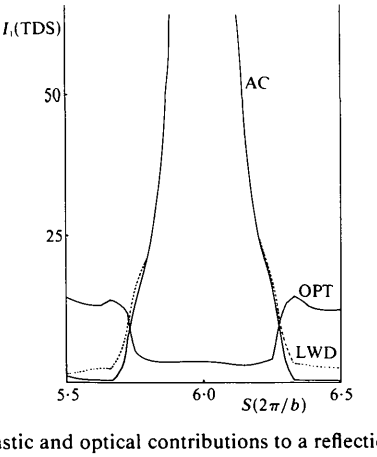

Fig. 2. Acoustic and optical contributions to a reflection along **b***.

Table 1. *Empircal factor η as a function of sampling density*

n	η
0	1·19
2	1·48
3	1·34
4	1·35
⋮	⋮
∞	1·38

Table 2. *Acoustic and optical contributions to Bragg peaks in units directly comparable with $\|F(\mathbf{G})\|^2$*

h	k	l	$\sin\theta/\lambda$	$\|\mathbf{F}(\mathbf{G})\|^2$	I_1(ac)	I_1(opt)
1	1	0	0·1074	266·2	2·794	−0·077
1	−1	−1	0·1101	3737·0	42·68	−0·063
2	−1	1	0·1753	229·7	6·180	−0·015
2	2	1	0·2282	39·31	2·072	−0·026
0	3	1	0·2576	436·6	25·43	−0·037
3	2	1	0·2756	69·91	4·126	−0·032
4	0	1	0·2833	577·4	40·91	−0·094
2	−4	−1	0·3609	18·70	2·236	−0·009
4	−3	2	0·3981	282·9	37·85	−0·024
3	3	4	0·4037	61·61	8·123	−0·028
6	1	1	0·4236	12·41	2·087	−0·066
3	−5	−2	0·4651	33·60	6·576	−0·009
7	−2	−3	0·4786	29·49	6·969	−0·033
8	2	−1	0·5474	14·68	4·446	−0·025
6	−4	2	0·5512	5·785	1·563	−0·018
7	5	−1	0·6398	6·329	2·326	−0·002
−5	6	−3	0·6438	5·618	2·013	−0·003
5	6	5	0·6857	1·251	0·501	−0·006
12	0	0	0·7981	0·0842	0·0472	−0·002
−8	7	7	0·8047	0·9212	0·5785	−0·001
7	7	7	0·8765	0·3885	0·2423	−0·001
0	0	20	0·9722	0·00032	0·00027	−0·000

well behaviour of the optical contribution through the Bragg reflection.

Correction of experimental intensities is usually made with a correction factor $\alpha_1(\mathbf{G})$ defined as the ratio between TDS contribution and Bragg contribution, so that

$$I_{\text{exp}}(\mathbf{G}) = I_{\text{Bragg}}(\mathbf{G})\{1+\alpha_1(\mathbf{G})\}.$$

In Table 3 we show factors $\alpha_1(\mathbf{G})$ calculated for a set of reflections using the exact calculation and the approximation LWD, and we can observe that, for large diffraction angles, the TDS contribution is important when compared with Bragg intensity and, on the other hand, correction factors calculated using the LWD approximation are very close to the exact values. This indicates that inside the parallelepiped the LW approximation holds, as can be seen in Fig. 3, which represents the deviation of the acoustic modes from the limit $q \ll$ along $\mathbf{b}^*$, where the anisotropy of intermolecular interactions makes the crystal show different dispersive behaviour depending on the directions of the polarization vectors of the various branches. For 7/25 $\mathbf{b}^*$, the limit of the parallelepiped, only branch 3 (Criado, Conde & Márquez, 1984) deviates appreciably. The deviation from the long-wave limit has been calculated as the absolute value of the product of the eigenvector for

Table 3. *Calculated correction factors $\alpha_1(\mathbf{G})$ for a set of reflections*

h	k	l	$\sin\theta/\lambda$	$\|F(\mathbf{G})\|^2$	$\alpha_1(\mathbf{G})$ (%)	$\alpha_1^{\text{LWD}}(\mathbf{G})$ (%)
1	1	1	0·1252	176·3	1·2	1·3
2	0	3	0·2228	89·60	3·3	3·8
−3	2	1	0·2555	147·3	6·7	6·3
3	−2	0	0·2612	177·6	6·2	6·3
4	1	0	0·2791	250·5	7·6	7·4
1	−3	−4	0·3148	240·9	8·8	8·9
2	4	−4	0·3937	149·2	14·1	14·4
1	5	−3	0·4451	5·274	17·2	17·7
−3	5	−2	0·4875	19·04	20·1	20·6
0	1	10	0·4934	71·65	19·4	19·8
4	−5	−3	0·4984	6·633	23·7	23·5
7	0	3	0·5248	1·968	23·9	23·8
5	5	5	0·6260	4·913	34·5	32·6
3	−7	−3	0·6272	5·214	35·7	35·8
9	2	1	0·6365	0·5038	31·0	37·4
10	1	−1	0·6588	12·96	41·9	42·3
5	1	10	0·6656	3·780	30·7	33·5
9	5	−4	0·7140	5·720	51·1	50·7
6	6	6	0·7513	0·6240	42·8	46·9
−6	−8	4	0·7806	0·8806	56·4	56·9
10	5	0	0·7875	0·2883	58·3	57·8
−7	−8	2	0·8101	1·790	61·4	60·6
7	8	6	0·9119	0·1041	70·1	70·3
0	11	7	0·9879	0·0189	85·1	85·2

a $\mathbf{q}$ vector and the eigenvector corresponding to the limit $q \ll$ along the same direction:

$$\text{Dev}\,(\mathbf{q}j_{ac}) = |\mathbf{e}(\mathbf{q}j_{ac}) \,.\, \mathbf{e}(\mathbf{q} \ll j_{ac})|.$$

Difference Fourier synthesis

In order to evaluate directly the effect that measured TDS intensity has over an electronic density map, we have followed a procedure analogous to that utilized by Kroon & Vos (1979). We have taken the energy-minimized structure, from which dispersion curves have been calculated, as the true one and calculated the experimental intensity, taking into account TDS contribution, observed in a hypothetical experiment by calculating the factors $\alpha_1(\mathbf{G})$ in the

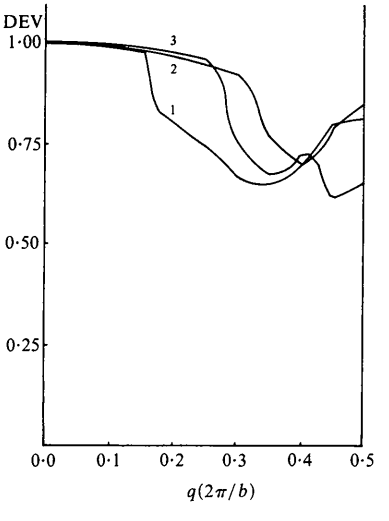

Fig. 3. Deviation of the acoustic modes from the LW approximation along $\mathbf{b}^*$.

long-wave approximation so as to save computational time. We have considered 1026 independent reflections, at 300 K, with $h<10$, $k<8$, $l<13$, $\sin\theta/\lambda<0{\cdot}6$ Å^{-1} and $\alpha_1(\mathbf{G})<37\%$. A Fourier synthesis (*FOURR* program; Stewart, Kundell & Baldwin, 1970) with coefficients $F_{exp}(\mathbf{G})-F_{true}(\mathbf{G})$, where $F_{true}(\mathbf{G})$ are the calculated structure factors of the minimized configuration, has been performed and its projection over a plane perpendicular to **b*** is shown in Fig. 4, where only positive density regions are represented, and black points correspond to the 'true' atomic positions. It can be seen that the effect of TDS contribution is to concentrate positive charge density around the atomic positions and therefore no important changes in atomic coordinates should be expected but, simultaneously, the difference map yields a negative density zone surrounding each positive peak, as can be seen in Fig. 5, showing the profile along of the S-atom peak. This usually means an undervaluation of the thermal crystallographic parameters

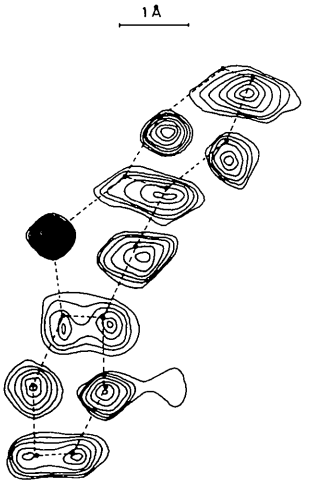

Fig. 4. Projection of difference electron density over a plane perpendicular to **b***. Contours are drawn at intervals of 0·06 e Å^{-2}.

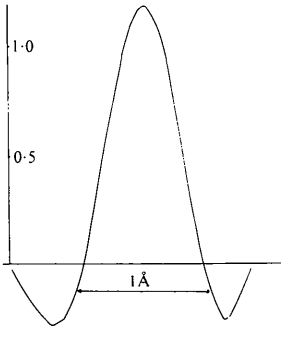

Fig. 5. Profile of S-atom peak in difference map along **a** in units of e Å^{-2}.

(Buerger, 1960), because its effect is a reduction of the time-averaged volume corresponding to each atom and, consequently, of the thermal parameters.

To verify this conclusion we have carried out a least-squares process (*CRYLSQ* program; Stewart, Kundell & Baldwin, 1970) with the 'experimental' intensities from the minimized structure and lattice-dynamical thermal parameters, where, in order to reduce the number of variables, thermal parameters for H atoms have been kept fixed.

$$\sum_{\mathbf{G}} \{|F_{exp}(\mathbf{G})| - k|F_{cal}(\mathbf{G})|\}^2$$

has been minimized and, after three cycles, changes in fractional coordinates were <0·001 for H atoms and 0·0001 for non-H atoms, within the e.s.d.'s in usual crystallographic studies. On the contrary, thermal parameters have decreased appreciably, about 10%, and the variation is almost equal for the different atoms in the molecule. This indicates that the effect of TDS intensity is most important on the rigid-body translation tensor **T**, a result that agrees with calculations performed by Kroon & Vos (1979). The scale factor k has changed from 1·00 to 0·997 and the agreement factor R from 6·4% at the beginning of the process to 0·02% at the end of it.

The great influence that first-order TDS intensity has over thermal parameters can be easily explained if we consider that the first-order intensity varies roughly as G^2 and that the correction factor multiplying I_{Bragg} is $1+\alpha_1(\mathbf{G})\sim\exp\{\alpha_1(\mathbf{G})\}$ if $\alpha_1(\mathbf{G})$ is small. Therefore, the effect of TDS intensity is equivalent to an artificial temperature factor adjustable in the least-squares process, and practically no influence is present over structural parameters. Second-order TDS intensity is approximately proportional to G^4 and, since it does not adjust to a temperature-factor functional form, it must be expected to have a greater influence on atomic coordinates.

It is our aim in the future to extend this computational method to the calculation of second-order TDS intensity and to study its influence on electronic density maps and structural parameters obtained in crystal structure analysis.

This work has been supported in part by the Spanish Government through the 'Comisión Asesora de Investigación Científica y Técnica'.

References

BELL, J. D., BLOUNT, J. F., BRISCOE, O. V. & FREEMAN, H. C. (1968). *Chem. Commun.* pp. 1656-1657.

BORN, M. & HUANG, K. (1968). *Dynamical Theory of Crystal Lattices.* Oxford: Clarendon.

BUERGER, M. J. (1960). *Crystal-Structure Analysis.* New York: Wiley & Sons.

BUSING, W. R. & LEVY, H. A. (1967). *Acta Cryst.* **22**, 457-464.
COCHRAN, W. (1963). *Rep. Prog. Phys.* **26**, 1-45.
COCHRAN, W. & PAWLEY, G. S. (1964). *Proc. R. Soc. London* **280**, 1-22.
CRIADO, A., CONDE, A. & MÁRQUEZ, R. (1984). *Acta Cryst.* A**40**, 696-701.
HELMHOLDT, R. B. & VOS, A. (1977). *Acta Cryst.* A**33**, 38-45.
International Tables for X-ray Crystallography (1974). Vol. IV. Birmingham: Kynoch Press. [Present distributor: D. Reidel, Dordrecht.]
KROON, P. A. & VOS, A. (1978). *Acta Cryst.* A**34**, 823-824.
KROON, P. A. & VOS, A. (1979). *Acta Cryst.* A**35**, 675-684.
MARADUDIN, A. A., MONTROLL, E. W., WEISS, G. H. & IPATOVA, I. P. (1971) *Theory of Lattice Dynamics in the Harmonic Approximation.* New York: Academic Press.
MARADUDIN, A. A. & VOSKO, S. H. (1968). *Rev. Mod. Phys.* **40**, 1-37.
STEWART, J. M., KUNDELL, F A. & BALDWIN, J. C. (1970). *XRAY70* system. Computer Science Center, Univ. of Maryland, College Park, Maryland.
VENKATARAMAN, G. & SAHNI, V. C. (1970). *Rev. Mod. Phys.* **42**, 409-470.
WILLIS, B. T. M. & PRYOR, A. W. (1975). *Thermal Vibrations in Crystallography.* Cambridge Univ. Press.

Acta Cryst. (1985). A**41**, 163-165

Image Processing in High-Resolution Electron Microscopy using the Direct Method. I. Phase Extension

BY FAN HAI-FU, ZHONG ZI-YANG, ZHENG CHAO-DE AND LI FANG-HUA

Institute of Physics, Chinese Academy of Sciences, Beijing, China

(*Received* 12 *June* 1984; *accepted* 8 *October* 1984)

Abstract

A procedure to combine the information from an electron micrograph (EM) and the corresponding electron diffraction (ED) pattern is proposed. Here the ED data will be used to obtain a set of amplitudes of the structure factors, while the EM will be used to obtain a set of starting phases assuming the weak-phase-object approximation. A direct method is then used to extend the phase information from a resolution of about 2 to 1 Å. The efficiency of the procedure has been verified by the test calculation on the model structure of copper perchlorophthalocyanine.

Introduction

The idea of combining the information from an EM and the corresponding ED pattern was first proposed by Gerchberg & Saxton (1971, 1972). They showed that the phase problem in both the image plane and the back focal plane can be solved by an iterative procedure. Later, Li (1977) reported the idea of improving the image resolution by the combination of EM and ED. Recently, Ishizuka, Miyazaki & Uyeda (1982) showed that, under the weak-phase-object approximation, improvement in both quality and resolution can be achieved by incorporating the phase correction method (summarized by Gassmann, 1976) into the combination of EM and ED. On the other hand, the application of the direct method, developed in X-ray crystallography, to the image deconvolution in high-resolution electron microscopy was proposed by Li & Fan (1979). This paper describes a procedure that makes use of the direct method in the combination of information from EM and ED. The method was tested under similar conditions assumed by Ishizuka *et al.* (1982).

Method

An ED pattern usually contains observable reflections within a limiting sphere of 1 $Å^{-1}$ radius. This implies that we can obtain from the ED data a structure image of about 1 Å resolution, which is considerably higher than that which can be reached by an EM. In addition, the intensities of the ED pattern from a crystalline specimen are independent of defocus and spherical aberration of the objective lens. Accordingly, under the weak-phase-object approximation,* a set of high-resolution structure amplitudes of good quality can be obtained from an ED pattern. However, the structure analysis by ED alone is subject to the well known difficulty of the 'phase problem'. On the other hand, an EM can provide phase information corresponding to about 2 Å resolution, which can greatly reduce the complexity of the solution of the phase problem. Hence, an improved high-resolution image may be obtained by a phase interpolation and extrapolation procedure using the amplitudes of the structure factors from ED and starting phases from EM.

* The applicability of the weak-phase-object approximation has been demonstrated by Unwin & Henderson (1975) for biological specimens and by Klug (1978/79) for an inorganic compound.

0108-7673/85/020163-03$01.50